

Variation in wind load and flow of a low-rise building during progressive damage scenario

Ahmed Elshaer^{*1}, Girma Bitsuamlak² and Hadil Abdallah²

¹Department of Civil Engineering, Lakehead University, 955 Oliver Rd, Thunder Bay, ON P7B 5E1, Canada

²Department of Civil & Environmental Engineering, Western University,
1151 Richmond St, London, ON N6A 3K7, Canada

(Received June 9, 2018, Revised January 20, 2019, Accepted February 28, 2019)

Abstract. In coastal regions, it is common to witness significant damages on low-rise buildings caused by hurricanes and other extreme wind events. These damages start at high pressure zones or weak building components, and then cascade to other building parts. The state-of-the-art in experimental and numerical aerodynamic load evaluation is to assume buildings with intact envelopes where wind acts only on the external walls and correct for internal pressure through separate aerodynamic studies. This approach fails to explain the effect of openings on (i) the external pressure, (ii) internal partition walls; and (iii) the load sharing between internal and external walls. During extreme events, non-structural components (e.g., windows, doors or roof tiles) could fail allowing the wind flow to enter the building, which can subject the internal walls to lateral loads that potentially can exceed their load capacities. Internal walls are typically designed for lower capacities compared to external walls. In the present work, an anticipated damage development scenario is modelled for a four-story building with a stepped gable roof. LES is used to examine the change in the internal and external wind flows for different level of assumed damages (starting from an intact building up to a case with failure in most windows and doors are observed). This study demonstrates that damages in non-structural components can increase the wind risk on the structural elements due to changes in the loading patterns. It also highlights the load sharing mechanisms in low rise buildings.

Keywords: low-rise building; wind load; aerodynamics; load sharing; progressive damage aerodynamics; turbulence, Large Eddy Simulation (LES); Computational Fluid Dynamics (CFD)

1. Introduction

During hurricanes and other extreme wind events, low-rise buildings are considered susceptible to wind damage. According to the report issued by NOAA (Smith *et al.* 2018), Hurricane Irma - September 2017 was responsible for the destruction of more than 25% of buildings in Florida, with 65% of the buildings experiencing significant damages, and 95 fatality incidents. It has been reported that the total damage cost due to climate disasters reported between 1980 to 2017 exceeds \$1.2 trillion (Smith *et al.* 2018). Numerous experimental and numerical studies are available in the literature investigating and assessing the behavior of low-rise buildings during extreme wind events. (Davenport 1977) conducted a series of wind tunnel tests for different low-rise buildings with different boundary layer wind profiles. (Lin *et al.* 1995) identified the critical corner regions by comparing wind tunnel results with existing full-scale measurements for different building heights and plan sizes. (Uematsu and Isyumov 1999) also reported many wind tunnel and field pressure measurements for building roofs. Many other studies were reported in the literature investigating wind loads on low-rise buildings adopting both experimental (Ginger and Holmes 2006,

Kopp *et al.* 2012, Teclé *et al.* 2015, Hajra *et al.* 2016) and numerical (Nozawa and Tamura 2002, Yang *et al.* 2008, Montazeri and Blocken 2013) methods. Furthermore, some studies introduced aerodynamic mitigation approaches as a way of reducing wind loads on low-rise buildings (Kopp *et al.* 2005, Bitsuamlak *et al.* 2012, Aly and Bresowar 2016). The focus of these studies was mainly towards examining the induced wind-loads on the external walls of the building, assuming intact building with a sealed envelope.

On the other hand, (Stathopoulos *et al.* 1979, Holmes 1980, Vickery and Bloxham 1992, Ginger *et al.* 1997) have carried out model-scale and full-scale studies to examine the mean and fluctuating internal pressures in buildings with openings and nominally sealed buildings. Afterward, (Ginger *et al.* 2008) expanded on the previous work by developing a cohesive relationship between internal pressures and external pressures at a dominant opening in terms of the sizes and volume of the opening. Moreover, (Ginger *et al.* 2010) studied the effect of roof suction along with the internal pressure on a dominant windward opening. An extensive literature review about the aerodynamics of low-rise buildings with openings was presented by (Holmes and Ginger 2012). A wind tunnel test was conducted by (Pan *et al.* 2013) on a one-story gable house model to investigate the progressive failure of openings and the effect of internal pressure. A detailed summary of the previous literature related to wind effect on low-rise buildings is summarized in Table 1.

*Corresponding author, Ph.D., P. Eng.
E-mail: aelshaer@lakeheadu.ca

Table 1 Scope and main findings of previous studies focused on wind effect on low-rise buildings

Reference	Method	Type of examined flow	Scope and main findings
(Davenport 1977)	BLWT	External	Examined different building geometries, showing the significance of the boundary layer flow and the effect of turbulence on structures
(Stathopoulos <i>et al.</i> 1979)	BLWT	Internal and external	Examined the wind-induced internal pressures using low-rise building models of different geometry and internal volume
(Holmes 1980)	BLWT	Internal and external	Examined the mean and fluctuating internal pressures in sealed buildings according to windward and leeward openings
(Vickery and Bloxham 1992)	BLWT	Internal and external	Studied internal pressures in buildings with large openings at model-scale
(Lin <i>et al.</i> 1995)	BLWT	External	Investigated the roof pressure distribution under the corner vortices and its variation with wind angle, building dimensions and turbulence.
(Ginger <i>et al.</i> 1997)	BLWT	Internal and external	Investigated the variation in mean and fluctuating internal pressure in a sealed building with changing windward/leeward open-area ratio
(Uematsu and Isyumov 1999)	Review Paper		Provided a detailed review of data for wind pressures acting on low-rise buildings, derived from various sources related to cladding design
(Nozawa and Tamura 2002)	CFD	External	Validated the large eddy simulation (LES) technique for predicting a flow around a typical low-rise building for a turbulent flow
(Stathopoulos 2003)	Review Paper		Provided an extensive review of evaluation of wind loads on low-rise buildings using both wind tunnel testing and CFD simulation
(Kopp <i>et al.</i> 2005)	BLWT	External	Examined different parapet geometries to mitigate loading on building non-structural components due to the formation of corner vortices.
(Ginger and Holmes 2006)	BLWT	External	Determined the external wind pressure distributions on large low-rise buildings with roof pitches of 15° and 35°
(Kopp <i>et al.</i> 2008)	BLWT	Internal and external	Investigated the effect of various openings on the internal pressure of a low-rise building by varying the size, ratio, leakage and location of the dominant openings
(Yang <i>et al.</i> 2008)	CFD	External	Validated the wind pressure distributions on a typical low-rise building using CFD and compared the results with BLWT
(Ginger <i>et al.</i> 2008) and (Ginger <i>et al.</i> 2010)	BLWT	Internal and external	Provided relationships between fluctuating internal pressures and the external pressure at a dominant wall opening, in terms of volume and dominant opening
(Kopp <i>et al.</i> 2012)	BLWT	Internal and external	Discussed the utilization of full-scale testing facilities (e.g., Three Little Pigs and large-scale wind tunnel) for enhancing the simulation of wind loads on low-rise buildings
(Holmes and Ginger 2012)	Review Paper		Provided an extensive review on fluctuating and peak internal pressures in buildings produced by a single dominant opening
(Bitsuamlak <i>et al.</i> 2012)	BLWT	External	Examined architectural elements as aerodynamic mitigation devices for reducing high wind-induced suctions at roof and wall corners
(Pan <i>et al.</i> 2013)	BLWT	Internal and external	Investigated the effect of building geometry and opening size on the internal pressure at each stage of a progressive failure
(Montazeri and Blocken 2013)	CFD	External	Determined the mean wind pressure coefficients on building facades with and without balconies
(Teclé <i>et al.</i> 2013, Teclé <i>et al.</i> 2015)	BLWT	Internal and external	Examined different dominant opening sizes and compartments and their effects on wind pressures on a low-rise gable roof building
(Aly and Bresowar 2016)	BLWT and CFD	External	Compared the performance of aerodynamic roof mitigation techniques / devices (edge optimization) in the reduction of roof uplift forces

Based on the previous work, it is evident that, the contribution of internal walls needs to be considered, along with the external walls, for wind load resistance of low-rise buildings. Especially with the possibility of wind breaching the building envelope due to sudden impact of wind-carried debris on non-structural components (e.g., window, door, roof tile) or by exceeding the wind load capacity of these components. Various damage states may result in (1) altering the wind flow field internally and externally, (2) redistributing wind loads on the external walls and roof, (3)

subjecting the internal walls to additional lateral loads, which are not typically considered in their structural design, and (4) exposing building surfaces (walls and roof) to a combination of both the internal and external pressures (i.e., net forces), which is the main concern of the current study.

The current work aims to investigate the change in wind flow and wind load distribution along both external and internal surfaces of the building under predetermined progressive failure scenario. The damage states are assumed based on a possible progressive collapse scenario, which is found to be satisfactory for investigating the changes in the

Table 2 Summary for cases naming and damage details

Case name	Damage stage	Angle of attack (AoA)	Failed windows	Failed doors
C0-00	C0	0°	--	--
C1-00	C1	0°	W1 in Story 2 (3.5% of total windows)	D1 in Story 2 (5% of total doors)
C2-00	C2	0°	W1 in all stories W2, W3 in Story 2 and roof window (24% of total windows)	D1 in all stories D2, D3 in Story 2 (30% of total doors)
C3-00	C3	0°	All in Stories 2, 3 and 4 W1, W4 in Story 1 and roof window (83% of total windows)	All in Stories 2, 3, 4 D1, D2, D3 in Story 4 (90% of total doors)
C0-45	C0	45°	--	--
C1-45	C1	45°	W1 in Story 2 (10% of total windows)	D1 in Story 2 (10% of total doors)
C2-45	C2	45°	W1 in all stories W2, W3 in Story 2 and roof window (24% of total windows)	D1 in all stories D2, D3 in Story 2 (10% of total doors)
C3-45	C3	45°	All in Stories 2, 3 and 4 W1, W4 in Story 1 and roof window (83% of total windows)	All in Stories 2, 3, 4 D1, D2, D3 in Story 4 (90% of total doors)

aerodynamics and load distributions for various damage stages. Typically, wind damage progresses due to many factors including the building layout, the capacity of openings (i.e., windows and doors) and upcoming wind characteristics. Thus, for a further realistic simulation, Computational Fluid Dynamic (CFD) can be coupled with structural modeling (e.g., finite element method) assigning the non-structural components to rupture when exceeding their load capacities. The study model is a four-story gable roof house examined for three damage stages in addition to the undamaged (or intact) case. CFD simulations are used to study the wind effect at the damage stages for two critical wind azimuths. In the first two stages, non-structural elements (i.e., windows and doors) in the windward face are assumed to be damaged allowing the wind to flow through the building envelope. While at the final stage, damages are assumed to propagate to the leeward face allowing the trapped flow to channel through the building. Wind-induced pressures and forces acting on walls (internal and external) and roof are evaluated. The paper is organized into four sections. Section 1 (this section) presents an introduction and literature review on the previous studies examining the wind effect on low-rise buildings. In Section 2, a description of the adopted CFD model is provided. Section 3 presents the results and discussion. Finally, Section 4 summarizes the conclusions and main findings of the study.

2. Numerical model details

2.1 Study case

The study building occupies a square footprint (20 x 20 meters) and consists of four stories of equal height (3 meters). The geometric details of the typical plan and

section elevation are shown in Fig. 1. The typical plan includes 7 windows and 5 doors, and the story plan is divided into 5 regions. The current study assumes a predefined progressive failure scenario, which is represented by four damage stages (i.e., C0, C1, C2 and C3). The damage stages and flow accessibility in each story is demonstrated in Fig. 2. For damage stage (C0), the building is considered intact with no wind flow allowed to enter the building envelope. The first damage stage (C1) is assumed to occur at the windward face due to the failure of the window (W1) allowing wind to access Zone 1 of Story 2. As the damage progresses to (C2), wind flow accesses Zones 1 and 2 in all stories due to the damage of windows (W1, D1 and roof window), while for Story 2, Zone 3 and 4 become accessible to wind due to the failure of (W2, W3, D2 and D3). As for the last damage stage (C3), almost all windows and doors (i.e., 83% of windows and 90% of doors) are assumed to be damaged allowing the wind to reach all the building zones. Damage aerodynamics are studied for two critical wind azimuths (i.e., 0° and 45°). A detailed summary for the damage stages and failed components are presented in Table 2.

2.2 Numerical simulation

Full-scale large eddy simulation (LES) models are utilized to simulate and assess the proposed progressive failure scenario described in the previous section. The computational domain dimensions are defined based on the recommendations of (Franke *et al.* 2007) and (Dagnew and Bitsuamlak 2013). A no-slip wall boundary condition is assigned to the ground and all walls of the building, while symmetry plane boundary condition is assigned for top and side faces of the computational domain.

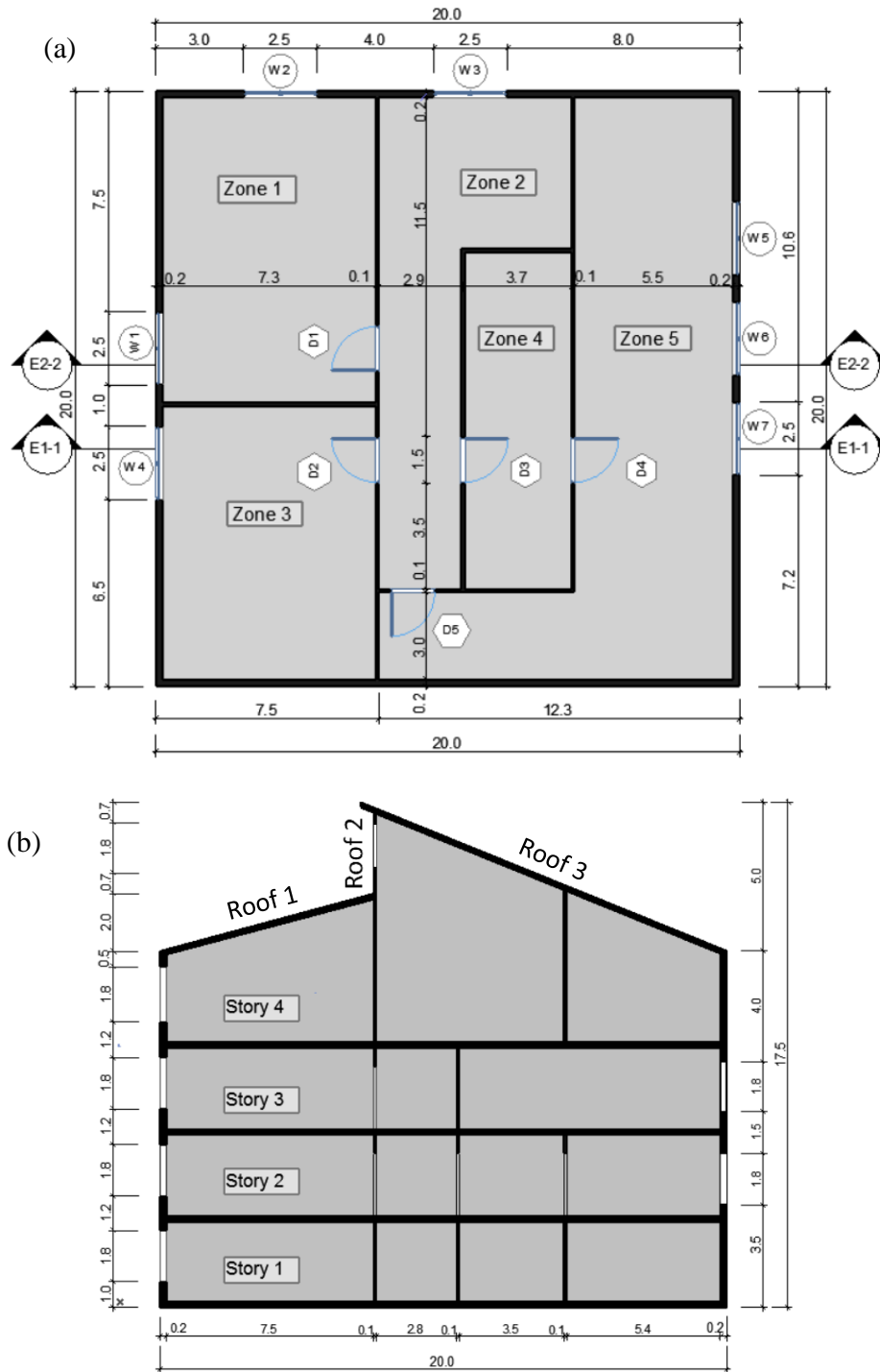


Fig. 1 (a) Typical Plan and (b) Section Elevation (E 1-1) dimensions (in meters) for the study building

The outflow of the computational domain is defined as a pressure outlet, while the inflow is defined using the Consistent Discrete Random Flow Generation (CDRFG) introduced by (Aboshosha *et al.* 2015). Fig. 3 shows the computational domain dimensions and the boundary conditions assigned for the LES. The profile for the mean, turbulence intensity and turbulence length scales are generated adopting an urban terrain exposure following the (ESDU 2001) guidelines (Fig. 4). The computational domain is discretized into hexahedral

meshes using the trimmer meshing algorithm for a total of 1.6M cells. The mesh size of 4.0 meters is selected for the region away from the study area at (Mesh Zone 1). The computational domain is further refined (i.e., mesh size = 0.2 meters) near the study building and in the region between the inlet and the building (Mesh Zone 2), so as to capture the generated turbulence from the inflow boundary condition and to maintain the Y^+ value around 1.0, as shown in Fig. 5. The time step is chosen to be equals to 0.05 seconds to maintain the

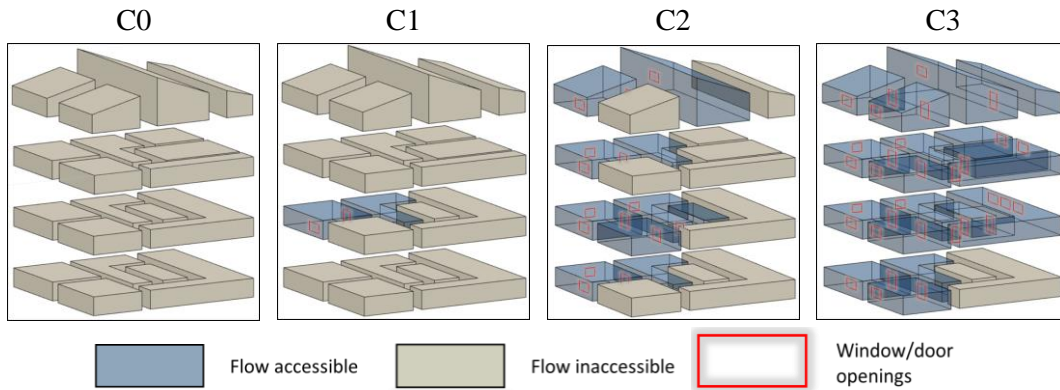


Fig. 2 Wind accessibility zones through damage stages

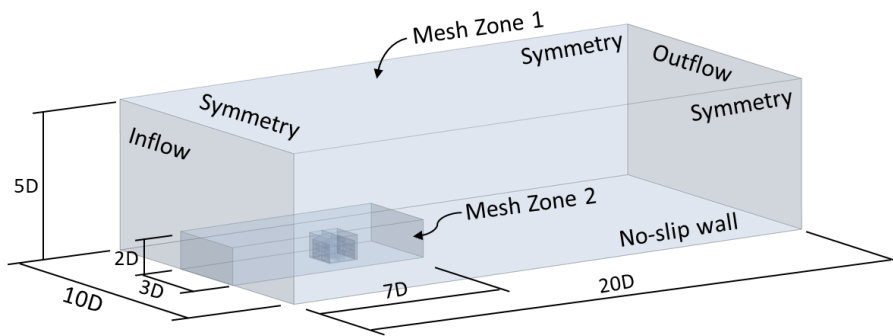


Fig. 3 Computational domain dimensions and boundary conditions

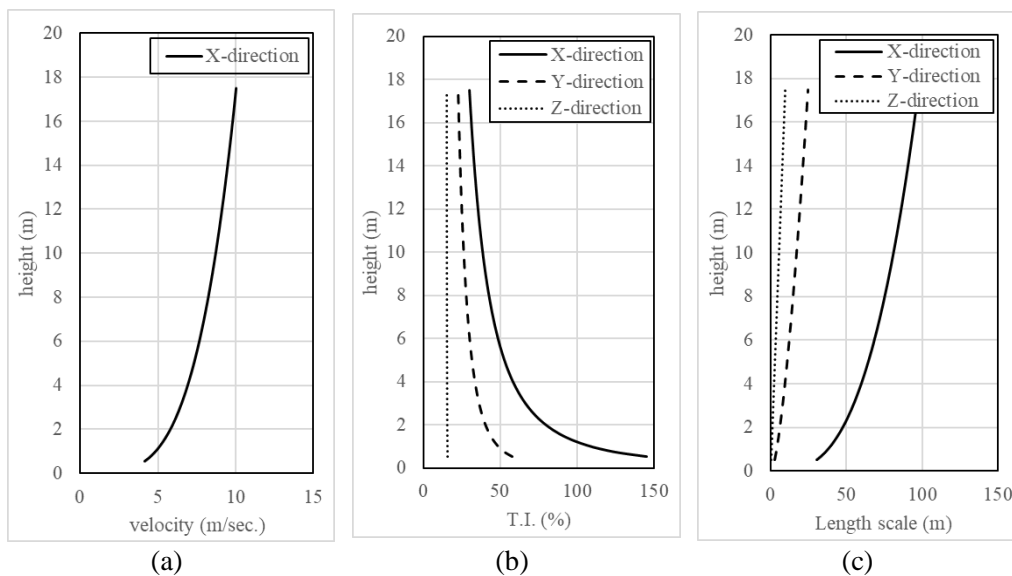


Fig. 4 (a) mean velocity, (b) turbulence intensity and (c) turbulence length scale profiles used for inflow generation using CDRFG technique

Courant number below 1.0 to ensure numerical convergence of the solver (Courant *et al.* 1928). The numerical simulations are conducted for 2,000 time-steps, which represent 100 seconds. The numerical model required 400 time-steps (i.e., 20 seconds) to reach statistical conversions, where this period was neglected in evaluating the aerodynamic results.

For the remaining 1600 time-steps, the results were extracted for all time steps (i.e., sampling frequency equals 1). The LES are conducted using (Star CCM+ v.10.02.011 2016) by employing a dynamic sub grid model proposed by (Smagorinsky 1963) and utilizing a coupled velocity-pressure solver. The CFD details including the adopted mesh resolution,

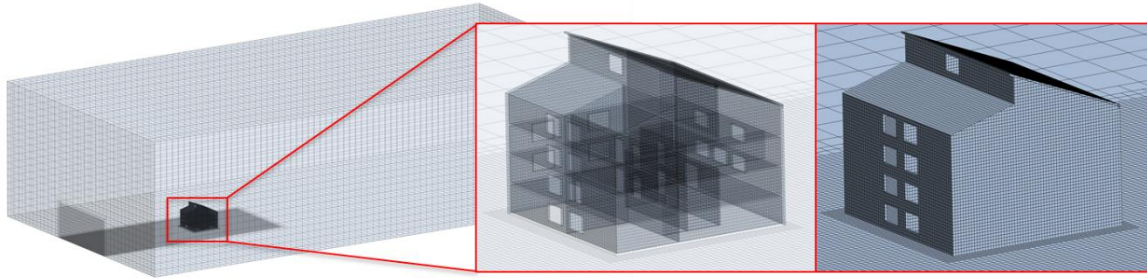


Fig. 5 Mesh grid resolution utilized in the CFD simulations

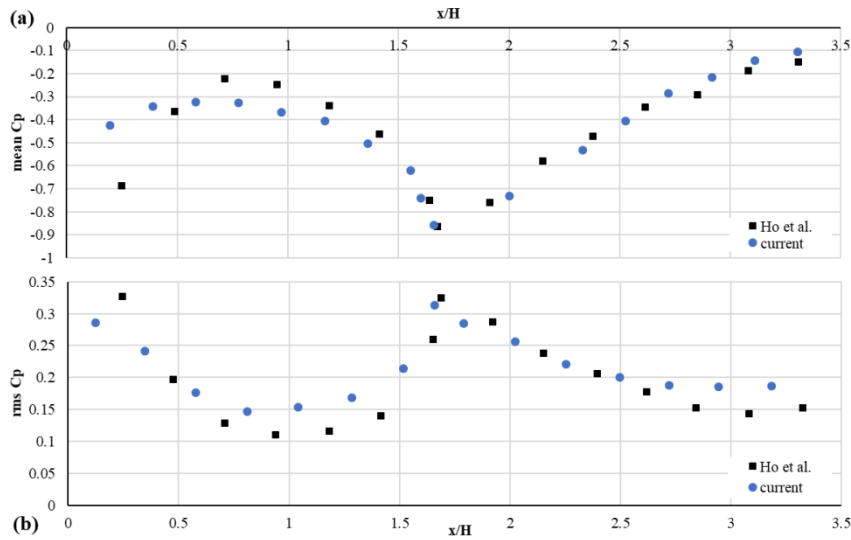


Fig. 6 Spatial variation of the (a) mean and (b) rms pressure coefficients along a line of taps at the middle of the building for a wind angle of 270°

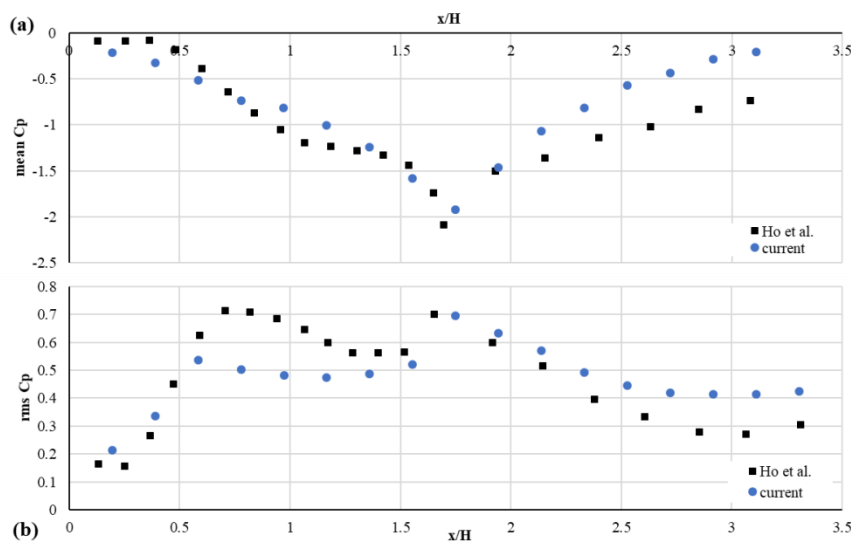


Fig. 7 Spatial variation of the (a) mean and (b) rms pressure coefficients along a line of taps at the middle of the building for a wind angle of 325°

the time discretization, the inflow generation and the solver characteristics are used assigned as per (Franke *et al.* 2007) and (Dagnew and Bitsuamlak 2013).

As a validation for the adopted CFD model, additional simulations are conducted for a low-rise building that is experimentally tested by (Ho *et al.* 2005) with a gable roof

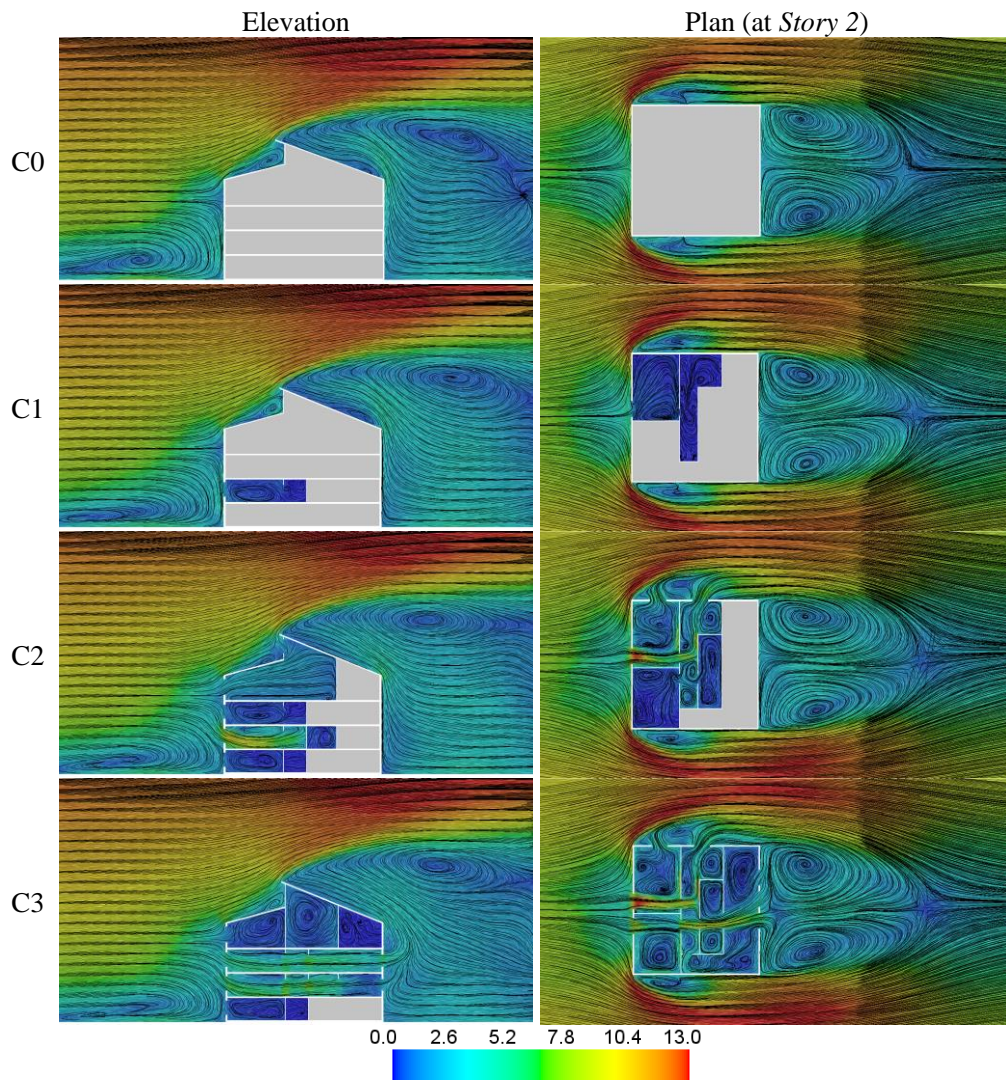


Fig. 8 Mean velocity contours and wind flow streamlines for different damage stages (AoA=0°)

(roof slope = 3/12; and eaves height = 7.32 meters) for two wind angles of attack (i.e., 270° and 325°). All aerodynamic and geometrical details in these validation models are assigned to match the experimental setup, including the building geometry and inflow characteristics. The mean and fluctuating pressure distributions obtained from the CFD agreed well with the wind tunnel tests (i.e., average error is 3.5%), as shown in Figs. 6 and 7. The discrepancy between the numerical and experimental work is attributed to the nature of extraction of pressure reading between CFD and wind tunnel.

3. Results and discussions

3.1. Wind flow field and pressure distribution

The mean wind velocity field and mean velocity streamlines are shown in Figs. 8 and 9 for cases of wind AoA equal to 0° and 45°, respectively. It can be noted that there are slight differences in the wind flow structure surrounding the building, especially for damage stage (C3), as the flows channelling through the study building,

disrupting the flow in the wake behind the building. On the contrary, the internal mean flows vary significantly across different damage levels. For instance, at Case C1-00, the incoming wind flow at Story 2 was trapped due to the opening of W1 and D1 forming a recirculation in Zone 1.

This entrapped flow is expected to cause high values of fluctuating forces on the internal walls surrounding it. As the damage progresses to (C2), the flow channels through the building and exiting the building through W3. As for (C3), two channelling flows are formed in both Story 1 and Story 2 where the wind enters through W1 and W4, and exit through W3 and W7, respectively. Regarding cases of AoA=45°, a similar internal flow is developed for (C1). While for (C2) and (C3), W2 and W3 are both on the windward faces of the building and the flow is entrapped inside (as opposed to forming channelling flow unlike cases of AoA=0°). Figs. 10 and 11 show the mean pressure coefficient (C_p) distributions for the cases of AoA equal to 0° and 45°, respectively. It can be observed that the mean C_p distributions on the external walls do not change significantly over different damage stages (i.e., less than 3.5%). However, rms C_p distributions on the external wall

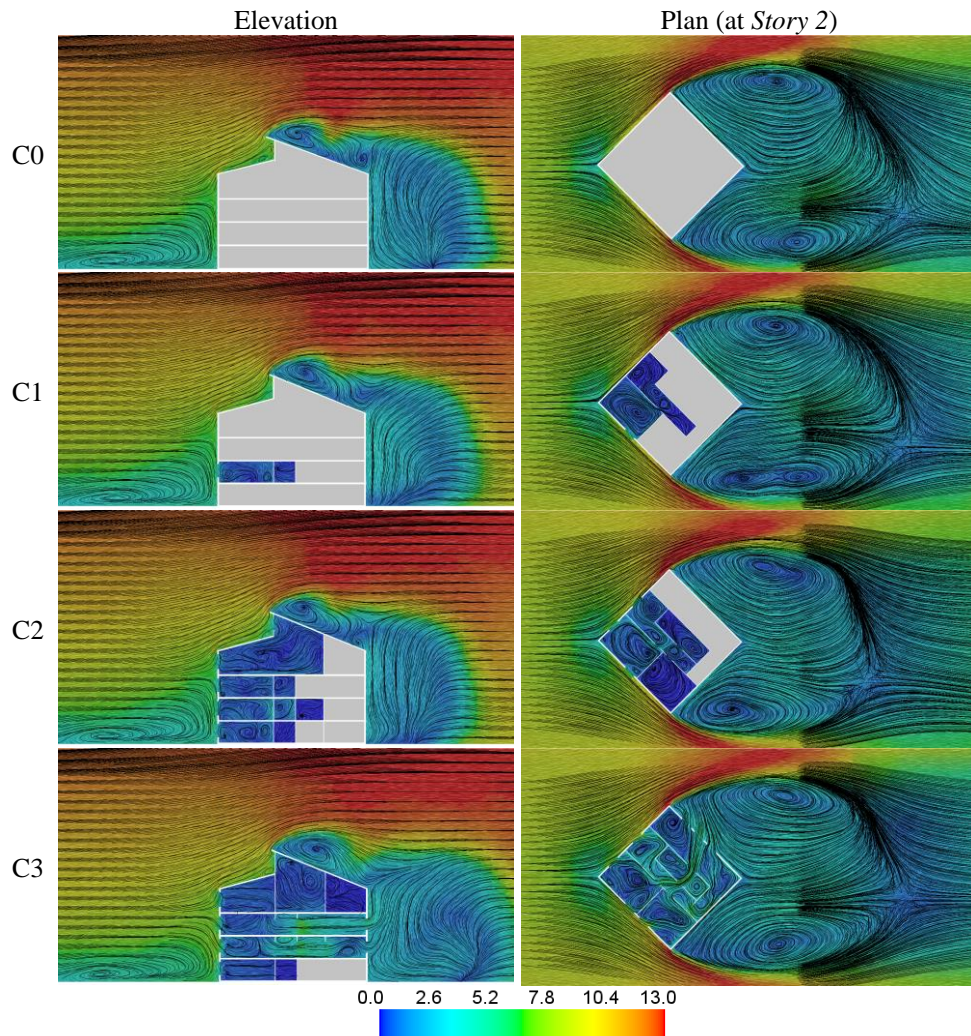


Fig. 9 Mean velocity contours and wind flow streamlines for different damage stages ($AoA=45^\circ$)

(Figs. 12 and 13) show low fluctuations in wind pressure for cases (C0 and C1) and the fluctuations increase as the building continues to be damaged (C2 and C3). During the assumed early damage stages, incoming turbulence and flow interaction with the buildings create large fluctuating components of both external and internal wall forces. Progressing to the later assumed damage stages, the channelling flow tends to reduce the fluctuating flow, which leads to a slightly reduced rms values.

3.2 Wind forces on walls and roof

The total foundation level wind forces (drag and lift) have been evaluated by integrating the wind pressures on both external and internal walls of the building. The drag force on wall is computed in the direction of the flow, while the lift force is computed in the perpendicular transversal direction to the flow. Figs. 14 and 15 show the total drag and lift forces acting on the building walls for cases of AoA equal to 0° and 45° , respectively. The figures show the mean forces on the external walls has not changed significantly with the change in the damage level (i.e. less than 3.0%) for both wind directions.

While the fluctuations component of wind forces on the external wall have been suppressed (i.e., up to 25% compared C0) as the building damage progresses. This can be attributed to the opposition of wake formation caused by the flow channelling through the building. A significantly high fluctuating component in the drag forces on the internal walls (i.e., ~ 1.5 times the corresponding external forces) can be observed in damage stage (C1), especially for the wind azimuth of 0° . The amplification of the fluctuating component of the internal wind forces is due to a flow resonance, which is known as ‘‘Helmholtz resonance’’ (Holmes 1980). As the building damage progresses, this high fluctuation in the drag forces decreases due to the release of the trapped flow through leeward openings, thus interfering with the flow circulation zones at the sides and wake. On the other hand, the lift force on the internal walls start to be significant (i.e., almost equivalent to the corresponding external forces) only after window damages on the side walls (e.g., W2 and W3) of the building (i.e., C2 and C3). Table 3 summarizes the mean, rms and peak wind forces on external and internal walls in Newtons (for reference velocity at the eave height = 10 m/s).

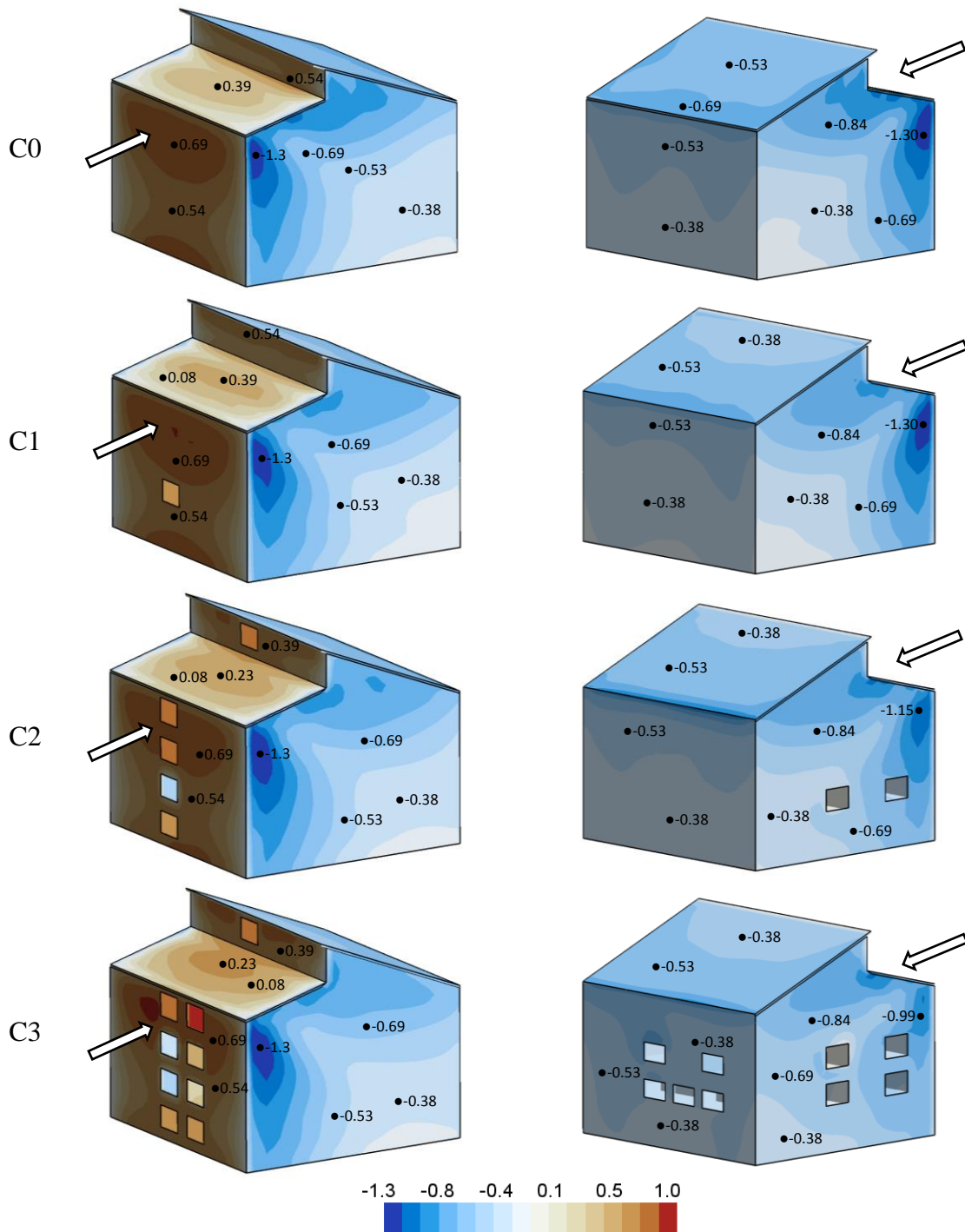


Fig. 10 Mean of Pressure Coefficient on external walls of the study building for different damage stages (AoA=0°)

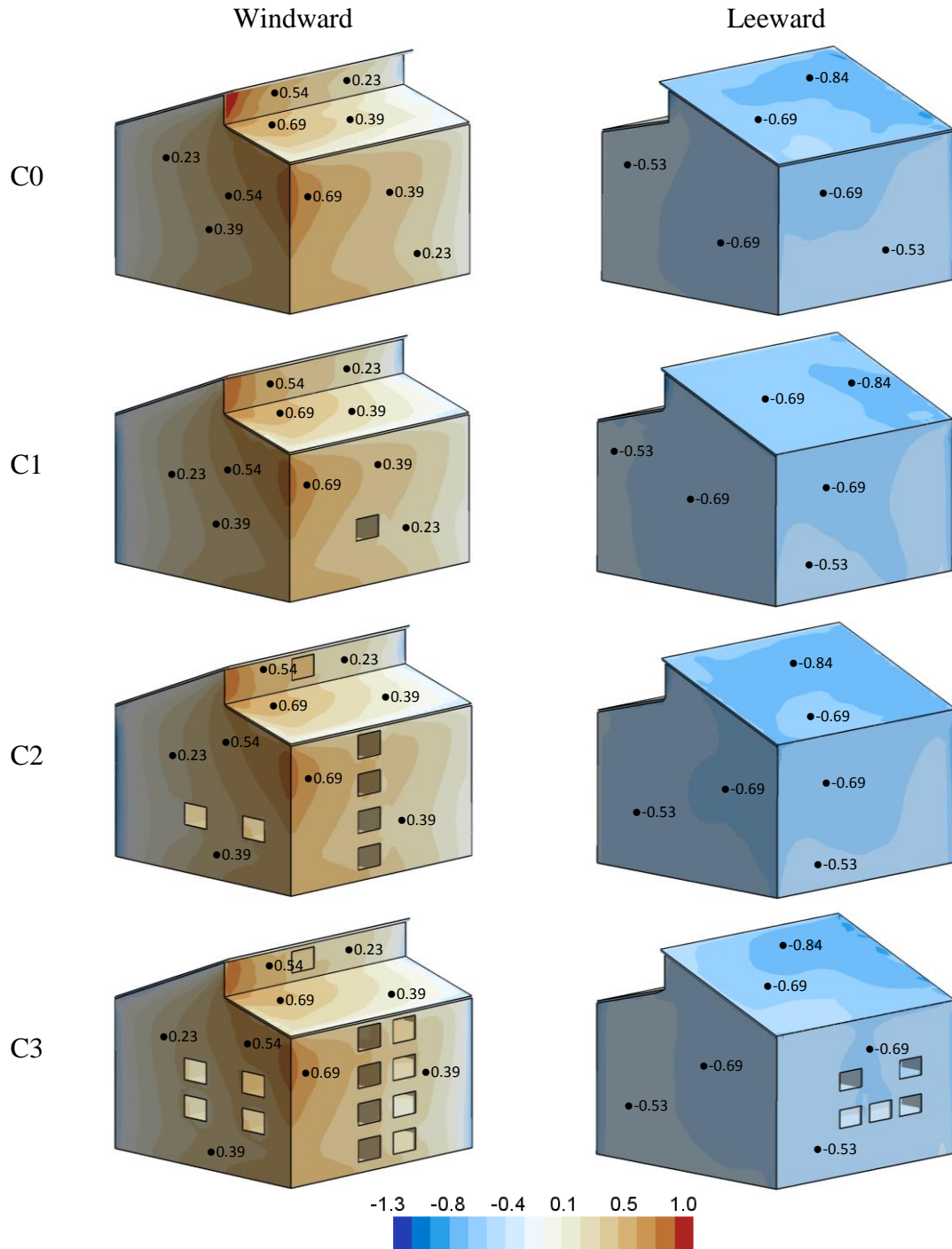


Fig. 11 Mean of Pressure Coefficient on external walls of the study building for different damage stages (AoA=45°)

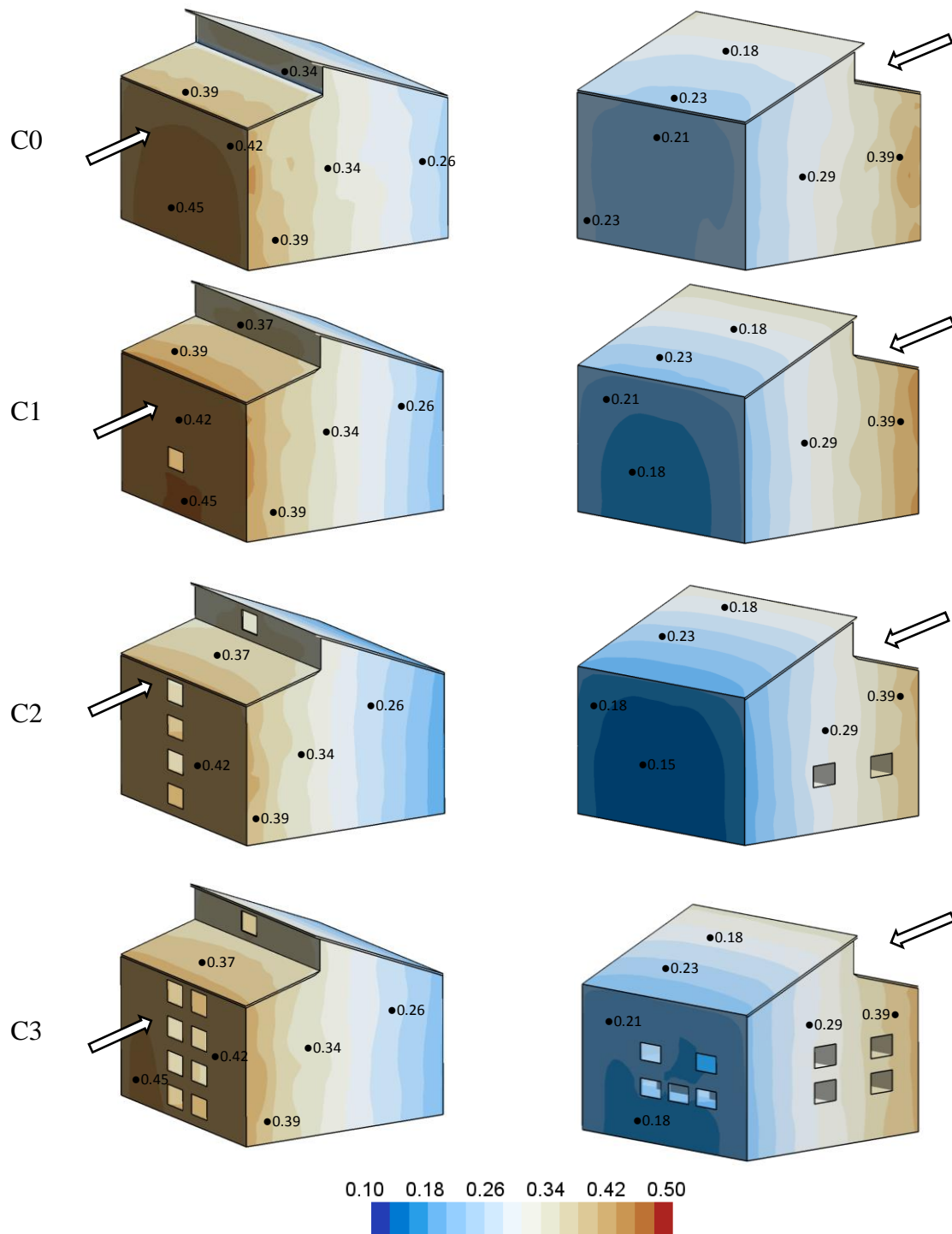


Fig. 12 RMS of Pressure Coefficient on external walls of the study building for different damage stages (AoA=0°)

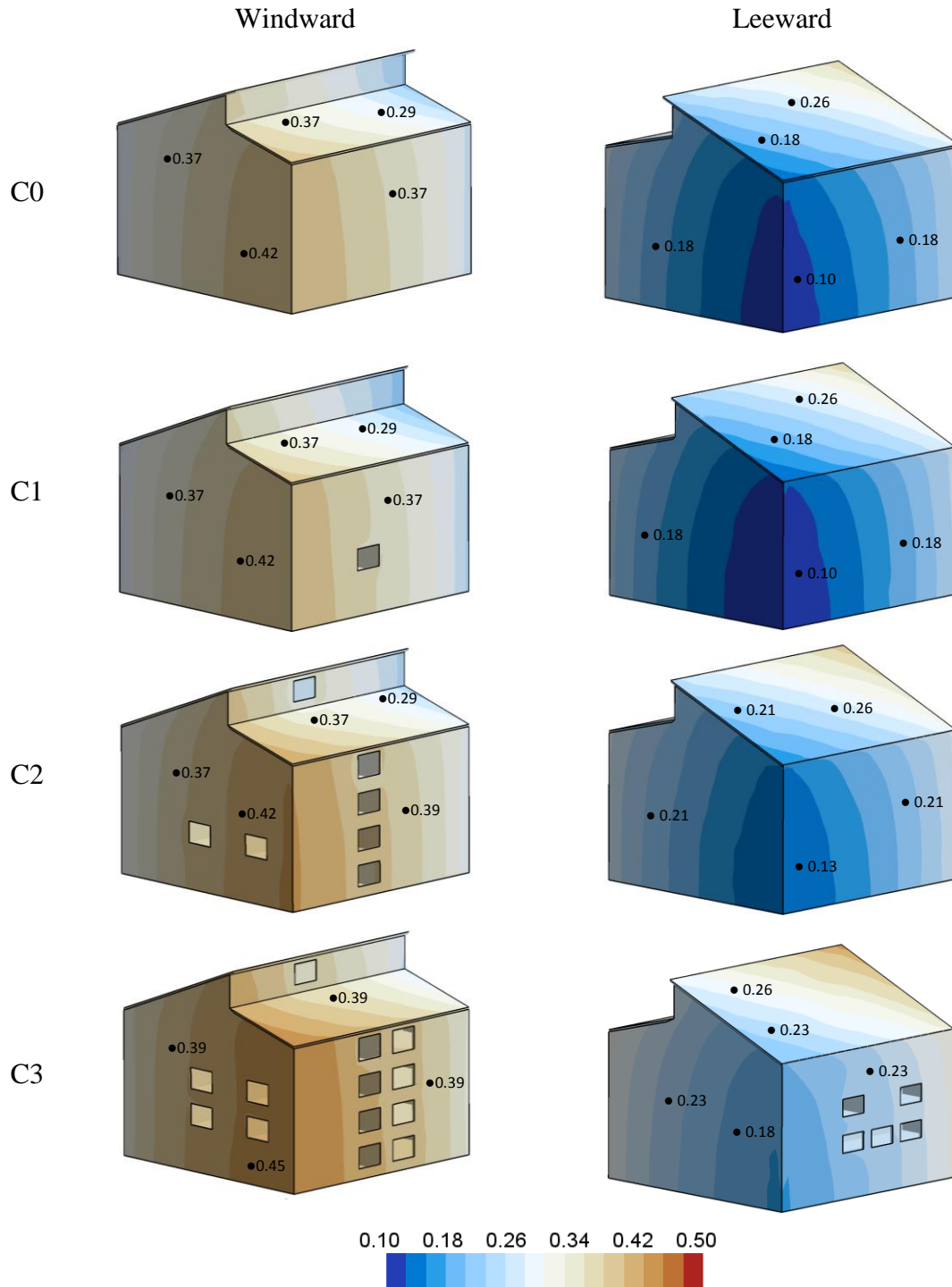


Fig. 13 RMS of Pressure Coefficient on external walls of the study building for different damage stages ($AoA=45^\circ$)

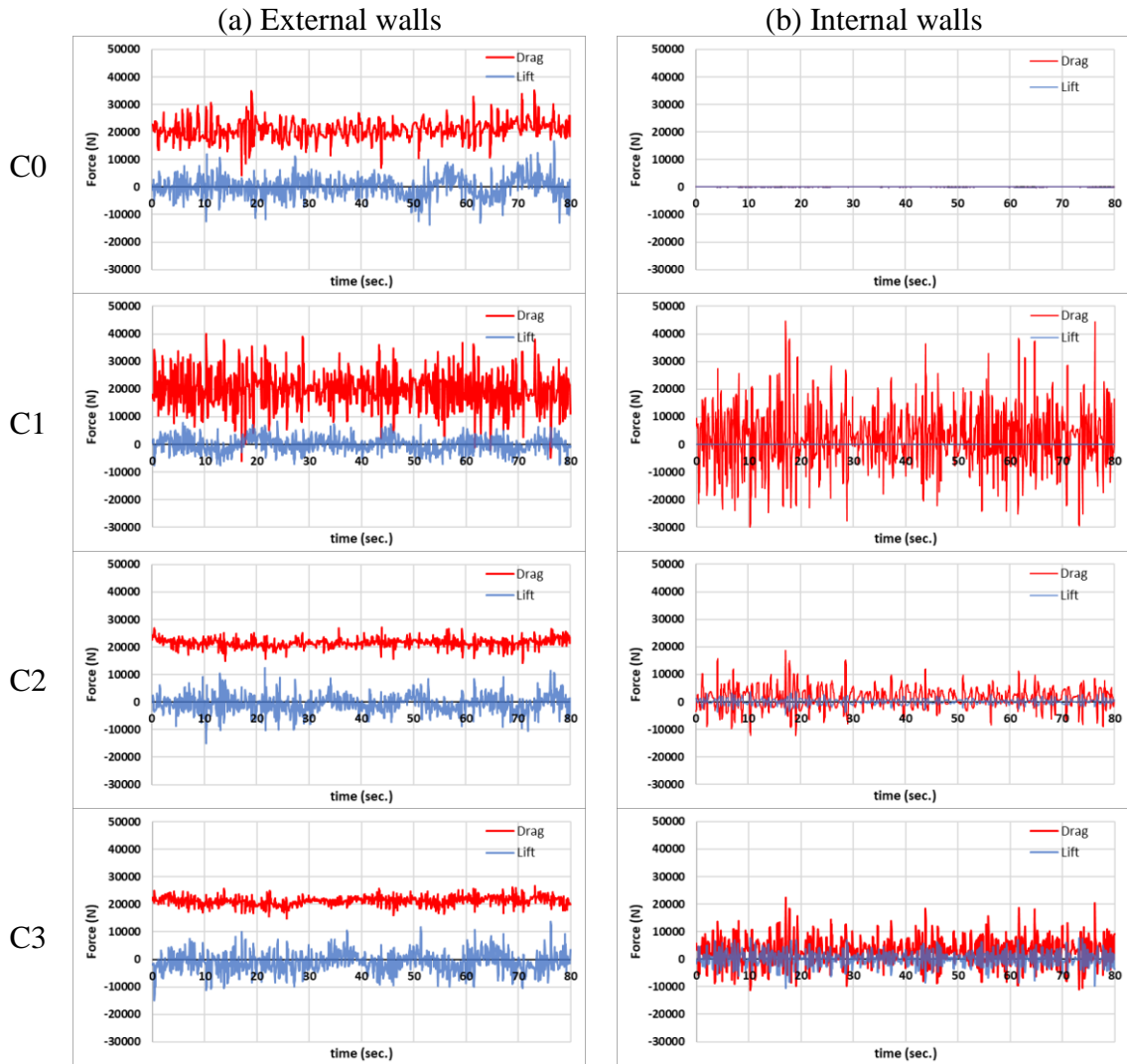


Fig. 14 Drag and lift forces time histories on the (a) external and (b) internal wall for different damage stages (AoA=0°)

The peak wind pressure is calculated using Eq. (1).

$$F_{peak} = F_{mean} + g_f \cdot F_{rms} \quad (1)$$

where g_f is the peak factor (assumed = 3.5)

Fig. 16 shows the time histories of roof forces (F1, F2 and F3) over the different damage stages for (AoA = 0°). When the building reaches damage stages C2 and C3, the internal pressure is found to alter the mean wind forces on Roof 1 and 2 (F1 and F2) from being positive stabilizing forces to negative uplift forces. In addition, the internal pressure inside the building increases the total uplift force on Roof 3 (F3) with the increase in building damage (i.e., up to ~1.9 times the maximum uplift force compared to the undamaged case C0). This is expected as both internal and external wind forces are acting in the same direction with respect to the roof. This increase in the developed uplift force on different parts of the roof indicates the potential increase in wind risk with the progression of building damage.

4. Conclusions

This study investigates the concept of varying aerodynamics and wind risk in relation to the progression in damage of non-structural components (i.e., windows and doors) of a typical low-rise building. The change in wind flow and wind-induced load throughout an assumed progressive failure scenario is highlighted by comparing an undamaged case to three different damage levels for two different wind incident angles (0° and 45°). The case studies explain the use of CFD-based approach to illustrate the changes in wind flow, in addition to assessing the change in wind pressure and load on walls (internal and external) and roof surfaces. As the building damage progresses, the wind flow entering the building envelope is found to subject the internal walls to an unanticipated design load case and increased cladding loads. This additional wind load case is found to increase both the mean and fluctuating components of the wind forces on the internal walls (up to 1.5 times the corresponding external wind forces) and roof (up to 1.9 times the maximum uplift force compared to the

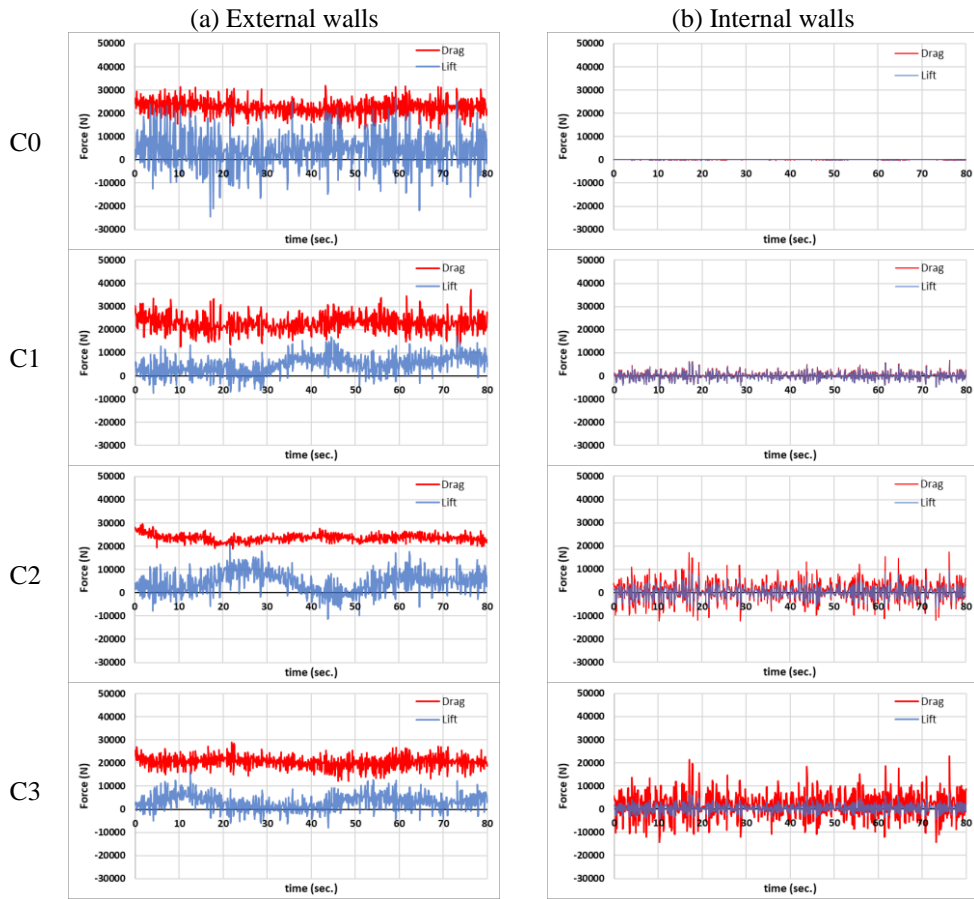


Fig. 15 Drag and lift forces time histories on the (a) external and (b) internal wall for different damage stages ($AoA=45^\circ$)

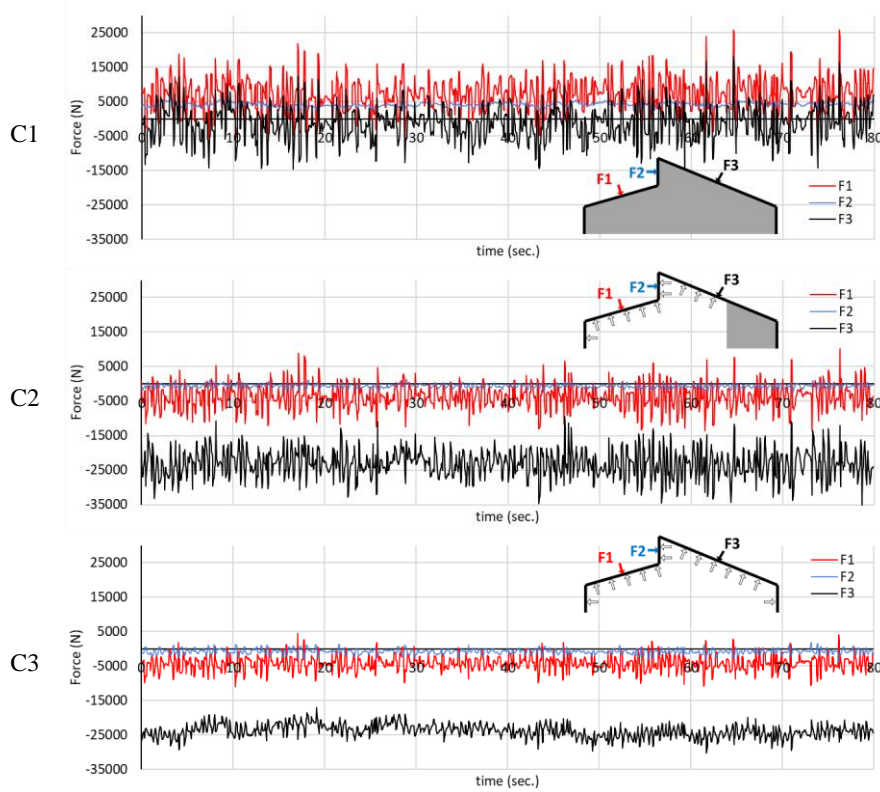


Fig. 16 Time histories of roof forces for different damage stages ($AoA=0^\circ$)

undamaged case C0). On the contrary, the development in building damage has a minor effect on both the wind flow around the building and the wind pressure on the external walls. In conclusion, the local damages of non-structural elements during wind events increase the wind risk on the overall structural elements (walls and roof), which illustrates the necessity of accounting for progressive collapse scenarios in the resilient structural design process. CFD-based simulations can be a useful tool that highlights the load sharing mechanism among various elements of building during the progression of building damage due to wind events. However, the exact impact of considering internal flow during the study of progressive damage depends on multiple parameters including the building layout, configuration of openings and inflow characteristics.

Acknowledgments

The authors would like to acknowledge the financial support from Ontario Center of Excellence (OCE), National Science and Engineering Research Center (NSERC), the Southern Ontario Smart Computing Innovation Platform (SOSCIP), and Canada Research Chair. The authors are grateful to SHARCNET and SCINET for access to high performance computing and for the support received from their excellent technical staff.

References

- Aboshosha, H., Elshaer, A., Bitsuamlak, G.T.G.T. and El Damatty, A. (2015), "Consistent inflow turbulence generator for LES evaluation of wind-induced responses for tall buildings", *J. Wind Eng. Ind. Aerod.*, **142**, 198-216. <https://doi.org/10.1016/j.jweia.2015.04.004>.
- Aly, A.M. and Bresowar, J. (2016), "Aerodynamic mitigation of wind-induced uplift forces on low-rise buildings: A comparative study", *J. Build. Eng.*, **5**, 267-276. <https://doi.org/10.1016/j.jobe.2016.01.007>.
- Bitsuamlak, G.T., Warsido, W., Ledesma, E. and Chowdhury, A.G. (2012), "Aerodynamic mitigation of roof and wall corner suction using simple architectural elements", *J. Eng. Mech.*, American Society of Civil Engineers, **139**(3), 396-408. [https://doi.org/10.1061/\(ASCE\)EM.1943-7889.0000505](https://doi.org/10.1061/(ASCE)EM.1943-7889.0000505).
- Courant, R., Friedrichs, K. and Lewy, H. (1928), "Über die partiellen Differenzgleichungen der mathematischen Physik", *Mathematische annalen*, **100**(1), 32-74.
- Dagnew, A. and Bitsuamlak, G.T. (2013), "Computational evaluation of wind loads on buildings: a review", *Wind Struct.*, **16**(6), 629-660. <http://dx.doi.org/10.12989/was.2013.16.6.629>.
- Davenport, A.G. (1977), *Wind Loads on Low Rise Buildings: Final Report of Phases I and II. Part I: Text and Figures*.
- ESDU. (2001), *Engineering Sciences Data Unit. Characteristics of atmospheric turbulence near the ground. Part II: single point data for strong winds*.
- Franke, J., Hellsten, A., Schlünzen, H. and Carissimo, B. (2007), "Best Practice Guideline for the CFD Simulation of Flows in the Urban Environment. COST Action 732: Quality Assurance and Improvement of Microscale Meteorological Models", Hamburg, Germany.
- Ginger, J.D. and Holmes, J.D. (2006), "Design wind loads on gable-ended low-rise buildings with moderate and steep roof slopes", *Australian J. Struct. Eng.*, **6**(2), 89-102. <https://doi.org/10.1080/13287982.2006.11464947>.
- Ginger, J.D., Holmes, J.D. and Kim, P.Y. (2010), "Variation of internal pressure with varying sizes of dominant openings and volumes", *J. Struct. Eng.*, **136**(10), 1319-1326. [https://doi.org/10.1061/\(ASCE\)ST.1943-541X.0000225](https://doi.org/10.1061/(ASCE)ST.1943-541X.0000225).
- Ginger, J.D., Holmes, J.D. and Kopp, G.A. (2008), "Effect of building volume and opening size on fluctuating internal pressures", *Wind Struct.*, **11**(5), 361-376. <https://doi.org/10.12989/was.2008.11.5.361>.
- Ginger, J.D., Mehta, K.C. and Yeatts, B.B. (1997), "Internal pressures in a low-rise full-scale building", *J. Wind Eng. Ind. Aerod.*, **72**, 163-174. [https://doi.org/10.1016/S0167-6105\(97\)00241-9](https://doi.org/10.1016/S0167-6105(97)00241-9).
- Hajra, B., Aboshosha, H., Bitsuamlak, G.T. and Elshaer, A. (2016), "Large eddy simulation of wind-induced pressure on a low rise building", Canadian Society of Civil Engineers, London, Canada.
- Ho, T.C.E., Surry, D., Morrish, D. and Kopp, G.A. (2005), "The UWO contribution to the NIST aerodynamic database for wind loads on low buildings: Part 1. Archiving format and basic aerodynamic data", *J. Wind Eng. Ind. Aerod.*, **93**(1), 1-30. <https://doi.org/10.1016/j.jweia.2004.07.006>.
- Holmes, J.D. (1980), "Mean and fluctuating internal pressures induced by wind", *Wind Eng.*, 435-450. <https://doi.org/10.1016/B978-1-4832-8367-8.50046-2>.
- Holmes, J.D. and Ginger, J.D. (2012), "Internal pressures—The dominant windward opening case—A review", *J. Wind Eng. Ind. Aerod.*, **100**(1), 70-76. <https://doi.org/10.1016/j.jweia.2011.11.005>.
- Kopp, G.A., Mans, C. and Surry, D. (2005), "Wind effects of parapets on low buildings: Part 4. Mitigation of corner loads with alternative geometries", *J. Wind Eng. Ind. Aerod.*, **93**(11), 873-888. <https://doi.org/10.1016/j.jweia.2005.08.004>.
- Kopp, G.A., Morrison, M.J. and Henderson, D.J. (2012), "Full-scale testing of low-rise, residential buildings with realistic wind loads", *J. Wind Eng. Ind. Aerod.*, **104-106**, 25-39. <https://doi.org/10.1016/j.jweia.2012.01.004>.
- Kopp, G.A., Oh, J.H. and Incelet, D.R. (2008), "Wind-induced internal pressures in houses", *J. Struct. Eng.*, **134**, 1129-1138. [https://doi.org/10.1061/\(ASCE\)0733-9445\(2008\)134:7\(1129\)](https://doi.org/10.1061/(ASCE)0733-9445(2008)134:7(1129)).
- Lin, J.X., Surry, D. and Tieleman, H.W. (1995), "The distribution of pressure near roof corners of flat roof low buildings", *J. Wind Eng. Ind. Aerod.*, **56**(2-3), 235-265. [https://doi.org/10.1016/0167-6105\(94\)00089-V](https://doi.org/10.1016/0167-6105(94)00089-V).
- Montazeri, H. and Blocken, B. (2013), "CFD simulation of wind-induced pressure coefficients on buildings with and without balconies: validation and sensitivity analysis", *Build. Environ.*, **60**, 137-149. <https://doi.org/10.1016/j.buildenv.2012.11.012>.
- Nozawa, K. and Tamura, T. (2002), "Large eddy simulation of the flow around a low-rise building immersed in a rough-wall turbulent boundary layer", *J. Wind Eng. Ind. Aerod.*, **90**(10), 1151-1162. [https://doi.org/10.1016/S0167-6105\(02\)00228-3](https://doi.org/10.1016/S0167-6105(02)00228-3).
- Pan, F., Cai, C.S. and Zhang, W. (2013), "Wind-induced internal pressures of buildings with multiple openings", *J. Eng. Mech.*, **139**(3), 376-385. [https://doi.org/10.1061/\(ASCE\)EM.1943-7889.0000464](https://doi.org/10.1061/(ASCE)EM.1943-7889.0000464).
- Smagorinsky, J. (1963), "General circulation experiments with the primitive equations: I. the basic experiment", *Mon. Weather Rev.*, **91**(3), 99-164. [https://doi.org/10.1175/1520-0493\(1963\)091<0099:GCEWTP>2.3.CO;2](https://doi.org/10.1175/1520-0493(1963)091<0099:GCEWTP>2.3.CO;2).
- Smith, A., Lott, N., Houston, T., Shein, K., Crouch, J. and Enloe, J. (2018), "US billion-dollar weather & climate disasters: 1980-2017", NOAA National Centers for Environmental Information accessed Jan 2018.
- Star CCM+ v.10.02.011. (2016), "CD-ADAPCO product. <www.cd-adapco.com/products/star-ccm+>", CD-ADAPCO Product.

- Stathopoulos, T. (2003), "Wind loads on low buildings: In the wake of Alan Davenport's contributions", *J. Wind Eng. Ind. Aerod.*, **91**(12-15), 1565-1585. <https://doi.org/10.1016/j.jweia.2003.09.019>.
- Stathopoulos, T., Surry, D. and Davenport, A.G. (1979), "Internal pressure characteristics of low-rise buildings due to wind action", JE Cermak, Wind Engineering, 1.
- Tecele, A.S., Bitsuamlak, G.T. and Aly, A.M. (2013), "Internal pressure in a low-rise building with existing envelope openings and sudden breaching", *Wind Struct.*, **16**(1), 25-46. <http://dx.doi.org/10.12989/was.2013.16.1.025>.
- Tecele, A.S., Bitsuamlak, G.T. and Chowdhury, A.G. (2015), "Opening and compartmentalization effects of internal pressure in low-rise buildings with gable and hip roofs", *J. Architect. Eng.*, **21**(1), 04014002. [https://doi.org/10.1061/\(ASCE\)AE.1943-5568.0000101](https://doi.org/10.1061/(ASCE)AE.1943-5568.0000101).
- Uematsu, Y. and Isyumov, N. (1999), "Wind pressures acting on low-rise buildings", *J. Wind Eng. Ind. Aerod.*, **82**(1), 1-25. [https://doi.org/10.1016/S0167-6105\(99\)00036-7](https://doi.org/10.1016/S0167-6105(99)00036-7).
- Vickery, B.J. and Bloxham, C. (1992), "Internal pressure dynamics with a dominant opening", *J. Wind Eng. Ind. Aerod.*, **41**(1-3), 193-204. [https://doi.org/10.1016/0167-6105\(92\)90409-4](https://doi.org/10.1016/0167-6105(92)90409-4).
- Yang, W., Quan, Y., Jin, X., Tamura, Y. and Gu, M. (2008), "Influences of equilibrium atmosphere boundary layer and turbulence parameter on wind loads of low-rise buildings", *J. Wind Eng. Ind. Aerod.*, **96**(10), 2080-2092. <https://doi.org/10.1016/j.jweia.2008.02.014>.